ASTRONOMY & ASTROPHYSICS
SUPPLEMENT SERIES

Astron. Astrophys. Suppl. Ser. **135**, 391–404 (1999)

V, *I* CCD photometry of metal-rich bulge globular clusters: NGC 6553⋆,⋆⋆

R. Sagar[1,2,3], A. Subramaniam[2], T. Richtler[2,3], and E.K. Grebel[4,5]

[1] U.P. State Observatory, Manora Peak, Naini Tal, India
e-mail: sagar@upso.ernet.in
[2] Indian Institute of Astrophysics, Bangalore 560034, India
e-mail: purni@iiap.ernet.in
[3] Sternwarte der Universität Bonn, Auf dem Hügel 71, D-53121 Bonn, Germany
e-mail: richtler@astro.uni-bonn.de
[4] Astronomisches Institut der Universität Würzburg, Am Hubland, D-97074 Würzburg, Germany
[5] University of California/Lick Observatory, Santa Cruz, CA 95064, U.S.A.
e-mail: grebel@ucolick.org

Received January 13; accepted October 2, 1998

Abstract. We have carried out VI CCD photometry of about 40 000 stars down to $V \sim 23$ mag in an area of about $6' \times 10'$ centered on the metal-rich Galactic bulge globular cluster NGC 6553 and an adjacent field region. Our photometry agrees fairly well with HST data. The cluster population dominates over the field population up to a radial distance of $\sim 3'$ from the cluster centre. The distance and reddening for the field population present in the direction of the cluster are derived for the first time. These values put the cluster NGC 6553 in the background of the young (age $\sim$ 800 Myr) Galactic disk stars but in the foreground of the old Galactic bulge populations. The similar values of $E(V-I) \sim 0.9$ for both the disk and the cluster indicate the absence of interstellar matter over a distance of ~ 3 kpc between the disk and the cluster. An analysis of the giant branch morphology confirms that the metallicity of the cluster population is similar to solar. The red giant branch (RGB) of both cluster and Galactic bulge extend beyond $(V-I) = 5$ and currently available theoretical isochrones reproduce its shape only up to $(V-I) \sim 4.5$. Our analysis indicates that the presence of differential interstellar extinction across the cluster face causes some elongation and tilt in the HB and produces scatter in the giant branch. The ratio of duration of the RGB-bump phase relative to the life time of the star during the HB phase derived from present observations is in good agreement with the theoretical predictions.

Key words: Galaxy: globular clusters: individual: NGC 6553 — Galaxy: abundances — stars: late-type — stars: horizontal branch — stars: abundances

1. Introduction

The Galactic bulge is a key component of our Galaxy. The study of the colour-magnitude diagram (CMD) of a Galactic bulge globular cluster is, therefore, valuable as it provides fundamental information about the cluster, such as its reddening, distance and chemical composition. These parameters play an important role in the understanding of formation and evolution of our Galaxy.

The Galactic bulge globular cluster NGC 6553 ≡ GCL 88 ($\alpha_{1950} = 18^{\rm h}06^{\rm m}11^{\rm s}$, $\delta_{1950} = -25°55'.1$, $l = 5.^{\circ}253$, $b = -3.^{\circ}029$), located in the direction of the Galactic centre belongs to metal-rich globular clusters (Zinn 1985). Structurally, it is a compact cluster with compactness parameter, $c = 1.17$ but it does not appear to be post-core-collapsed (Trager et al. 1995). It has a core radius of about $0.6'$ and radial velocity of -27 km s^{-1}. An inspection of sky survey plates indicates that the cluster is in a patchy and heavily obscured zone. Reddening determinations for the cluster vary from $E(B-V) = 0.7$ to 1.0 mag, while its estimated distance ranges from 3 to 6 kpc (Hartwick 1975; Ortolani et al. 1990, 1995; Guarnieri et al. 1998). The metallicity of NGC 6553 is close to solar

Send offprint requests to: R. Sagar, Naini Tal

⋆ Based on observations obtained under programme 51.5-0044 at the European Southern Observatory, La Silla, Chile.

⋆⋆ Table 2 only available in electronic form at the CDS via anonymous ftp to cdsarc.u-strasbg.fr (130.79.128.5) or via http://cdsweb.u-strasbg.fr/Abstract.html

([Fe/H] = -0.2 ± 0.4; Barbuy et al. 1992; Bruzual et al. 1997; Guarnieri et al. 1998 and references therein). Radial velocity and distance parameters of the cluster indicate that it is indeed a member of the Galactic bulge.

Hartwick (1975) presented a photographic BV diagram with an accuracy of ~ 0.1 to 0.2 mag in V up to $V \sim 18$ mag. Lloyd Evans & Menzies (1973) obtained instrumental VI photographic diagram for the cluster. But the usefulness of photographic data in such a crowded stellar field is very limited. Ortolani et al. (1990) have done a detailed $BVRI$ CCD photometric study of the cluster by observing about 15 000 stars down to $V = 21.5$ mag. They derived the cluster parameters and also indicated the presence of differential extinction across the cluster face. Recently, Guarnieri et al. (1995, 1998) have studied the cluster by combining the optical data with near-IR photometry. These studies indicate

(a) presence of some peculiar features in CMDs of the cluster e.g. curved giant branch (GB), which Ortolani et al. (1990) attribute to strong blanketing in the atmosphere of the metal-rich stars of the cluster. They even locate the red giant branch (RGB) tip at a V-band brightness comparable to the horizontal branch (HB);
(b) an anomalously tilted and very red HB; and
(c) a nearly solar abundance for NGC 6553.

The cluster is projected against a rich stellar background affected by differential extinction but in the photometric studies carried out so far the RGB and the HB of the cluster were not corrected for field star contamination. To understand the above mentioned peculiar features in the CMD of NGC 6553 it is important to consider that the cluster may be at the upper end of the metallicity scale of Galactic globular clusters. In 1993 we obtained a new set of better quality VI CCD images for the cluster region as well as for an adjacent field region. While we were still analysing the observations, Ortolani et al. (1995) published HST observations of NGC 6533, showing unambiguously the main-sequence turn-off (MSTO) location. They estimated an age of 12 ± 2 Gyr, which places NGC 6553 among the old Galactic globular clusters. Although the present data are the deepest obtained so far from the ground for NGC 6553, they are definitely not reliable for determining the location of the MSTO, especially in the presence of the superior HST data. We have therefore not made any attempt either to derive the cluster age or to discuss about the location of MSTO from the present data.

In this work, VI CCD photometry for more than 40 000 stars down to $V = 23$ mag in a field of about 6×10 arcmin^2 is presented. The data have been used to derive photometric parameters of the cluster and to present, for the first time, a cluster sequence corrected for the field star contamination. Reddening and distances to the field populations present in the direction of NGC 6553 are also estimated for the first time. The observations, data reduction and determination of metallicity, reddening and distance are described in the sections to follow.

Table 1. Observing log of CCD observations. Both cluster and field regions were observed on 1993 July 19

Region	Filter	Exposure in seconds	No. of frames	Airmass
Cluster	V	10	1	1.003
	V	30	3	1.004
	V	180	3	1.03
	I	30	1	1.009
	I	180	4	1.025
Field	V	180	4	1.065
	I	30	1	1.09
	I	180	3	1.15

2. Observations and data reduction

The observations were carried out with the 2.2-m MPIA telescope at the European Southern Observatory (ESO), La Silla, Chile, on the 19th of July 1993 using a 1024×1024 pixels^2 Thomson CCD (ESO # 19) detector attached to the ESO Faint Object Spectrograph and Camera (EFOSC II). A pixel of this CCD corresponds to 0.332 arcsec on the sky resulting in a field of view of $5.7' \times 5.7'$ at the Cassegrain focus of the telescope. ESO filters 584 (Bessell V) and 618 (Gunn i) were used for the observations. Table 1 gives a log of the observations. Figure 1 shows the identification chart for both cluster and field regions. The field region is located $\sim 4'$ south to the cluster and has an overlap of $\sim 1.5'$ with the cluster region. During the observations sky conditions were of good photometric quality and the seeing was better than $1''$. All observations were carried out when targets were close to zenith.

Sixteen stars from the list of Landolt (1992) were repeatedly observed for the photometric calibration. They cover a sufficient range in brightness ($13 < V < 16$) as well as in colour ($0.2 < (V - I) < 2.5$).

Twilight flat fields were used for all flat fielding. All photometric reductions were done using the DAOPHOT profile fitting programme (Stetson 1990, 1992). Further processing and conversion of these raw instrumental magnitudes to the standard photometric system were performed using the procedure outlined by Stetson (1992).

In deriving the colour equation for the CCD system and evaluating the zeropoints for the data frames, nightly values of atmospheric extinction were used. Further details of the data reduction can be found in our earlier paper on NGC 6528 (cf. Richtler et al. 1998), which was observed during the same run. We have therefore used the same colour equations for transforming the CCD instrumental magnitudes to standards ones. For establishing the local standards in both cluster and field regions, we selected

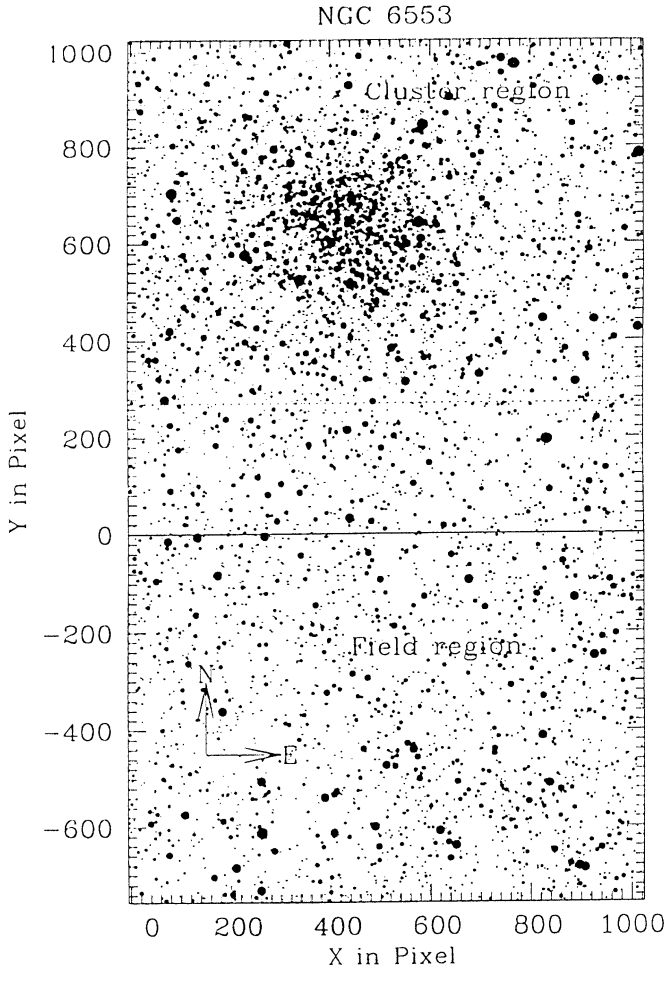

Fig. 1. Identification map for both cluster and field regions of NGC 6553. East and north directions are marked. The (X, Y) coordinates are in pixel units and one pixel corresponds to $0.332''$ on the sky. Filled circles of six sizes (each corresponding to one magnitude range in V) are used to represent brightness of the stars. Largest and smallest sizes denote stars in the brightest and faintest magnitude range of $V = 13$ to 14 and 18 to 19 respectively

about 40 stars on their reference frames, which according to brightness and the absence of close neighbours could serve as "secondary standards" in the sense of Stetson's calibration procedures. Using these local standards, the CCD profile magnitudes were transformed to the standard system. In this way, cluster and field regions are calibrated independently. The zeropoint accuracy of the colour equation is ~ 0.02 mag in V and ~ 0.01 mag in I. In addition to this, uncertainties in shutter timing and in correction between profile and aperture magnitudes, etc will also contribute to the final accuracy of our photometry. Also the accuracy of relative photometry is largely dominated by crowding and therefore it is a function of the relative position with respect to cluster centre. The internal errors estimated from the DAOPHOT programme are function of brightness. As expected, they increase with decreasing brightness. For brighter stars ($V \leq 18$), it is ~ 0.02 mag but becomes ≥ 0.2 mag near the limiting magnitudes of our observations. So the measurements of faintest magnitude bin in a region are not very reliable.

For all the stars observed in both cluster and field regions, the X and Y pixel coordinates, V and $(V - I)$ photometric magnitudes and their DAOPHOT errors and image parameters (χ and sharpness) along with number of measurements in V and I are given in Table 2, which is available only in electronic form at the CDS in Strasbourg. We have given only average V and $(V - I)$ values for stars common to both cluster and field regions in the combined data table, as the stars present in the overlapping regions show excellent agreement (within $0.01 - 0.02$ mag) between their VI values.

3. Comparison with previous measurements

In this section, we compare the present VI CCD data with the available photographic and CCD data. The difference (Δ) is always in the sense present minus others.

3.1. Photographic data

BV photographic observations were published by Hartwick (1975) up to $V \sim 18$ mag with a zeropoint accuracy of ~ 0.1 to 0.2 mag in V. Statistical results of the photographic V magnitude comparison are given in Table 3. The differences are a function of brightness as also pointed out earlier by Ortolani et al. (1990). However, they are within the uncertainty present in the photographic measurements.

3.2. CCD data

Ortolani et al. (1990) have carried out $BVRI$ CCD photometry of the cluster region using a detector whose sensitivity varied across the chip. The accuracy limits of their photometric calibration range from 0.07 to 0.15 mag. A comparison of their V and $(V - I)$ data with ours could be carried out as S. Ortolani kindly provided us with a computer-readable table of their photometric results. The transformation equations relating their ($X_{\rm Or}$, $Y_{\rm Or}$) coordinate system to ours ($X_{\rm pres}$, $Y_{\rm pres}$) are found to be,

$$X_{\rm Or} = -268.503 + 1.431 X_{\rm pres} - 0.007 Y_{\rm pres}$$

$$Y_{\rm Or} = -379.783 + 0.007 X_{\rm pres} + 1.431 Y_{\rm pres}.$$

There are 1150 stars in the Ortolani et al. (1990) data whose positions coincide within 1 pixel with the stars measured by us. The differences between the data sets are plotted in Fig. 2 and their statistical results are given in Table 3. A photometric comparison of the stars common between field and cluster regions is also shown in the figure

Table 3. Statistical results of the difference Δ in the sense present minus Ortolani et al. (1990) CCD and Hartwick (1975) photographic values. V and $(V-I)$ are from the present photometry. The mean and standard deviations (σ) are based on N stars. A few points discrepant by more than 3σ have been excluded

Ortolani et al. (1990) VI CCD data							Hartwick (1975) V data					
V	ΔV			$\Delta(V-I)$			$(V-I)$	$\Delta(V-I)$			V	ΔV		
(mag)	Mean	$\pm$	σ	N	Mean	$\pm$ σ	N	(mag)	Mean	$\pm$ σ	N	(mag)	Mean	$\pm$ σ	N
$14.0-16.0$	0.27	$\pm$	0.008	105	0.21	$\pm$ 0.01	107	$0.5-1.5$	0.16	$\pm$ 0.02	43	$15.0-15.5$	0.10	$\pm$ 0.10	8
$16.0-16.5$	0.26	$\pm$	0.008	68	0.21	$\pm$ 0.01	71	$1.5-1.8$	0.15	$\pm$ 0.02	60	$15.5-16.0$	-0.03	$\pm$ 0.13	16
$16.5-17.0$	0.27	$\pm$	0.008	263	0.20	$\pm$ 0.01	274	$1.8-2.0$	0.20	$\pm$ 0.01	122	$16.0-16.5$	-0.14	$\pm$ 0.12	13
$17.0-17.5$	0.27	$\pm$	0.008	153	0.20	$\pm$ 0.01	160	$2.0-2.2$	0.20	$\pm$ 0.01	461	$16.5-17.0$	-0.18	$\pm$ 0.13	67
$17.5-18.0$	0.28	$\pm$	0.009	164	0.20	$\pm$ 0.01	171	$2.2-2.4$	0.22	$\pm$ 0.01	207	$17.0-17.5$	-0.14	$\pm$ 0.16	35
$18.0-18.5$	0.30	$\pm$	0.01	159	0.22	$\pm$ 0.01	162	$2.4-2.6$	0.25	$\pm$ 0.01	108	$17.5-18.0$	-0.09	$\pm$ 0.12	19
$18.5-19.0$	0.30	$\pm$	0.01	128	0.23	$\pm$ 0.02	134	$2.6-7.0$	0.24	$\pm$ 0.01	110	$18.0-18.5$	0.06	$\pm$ 0.12	7

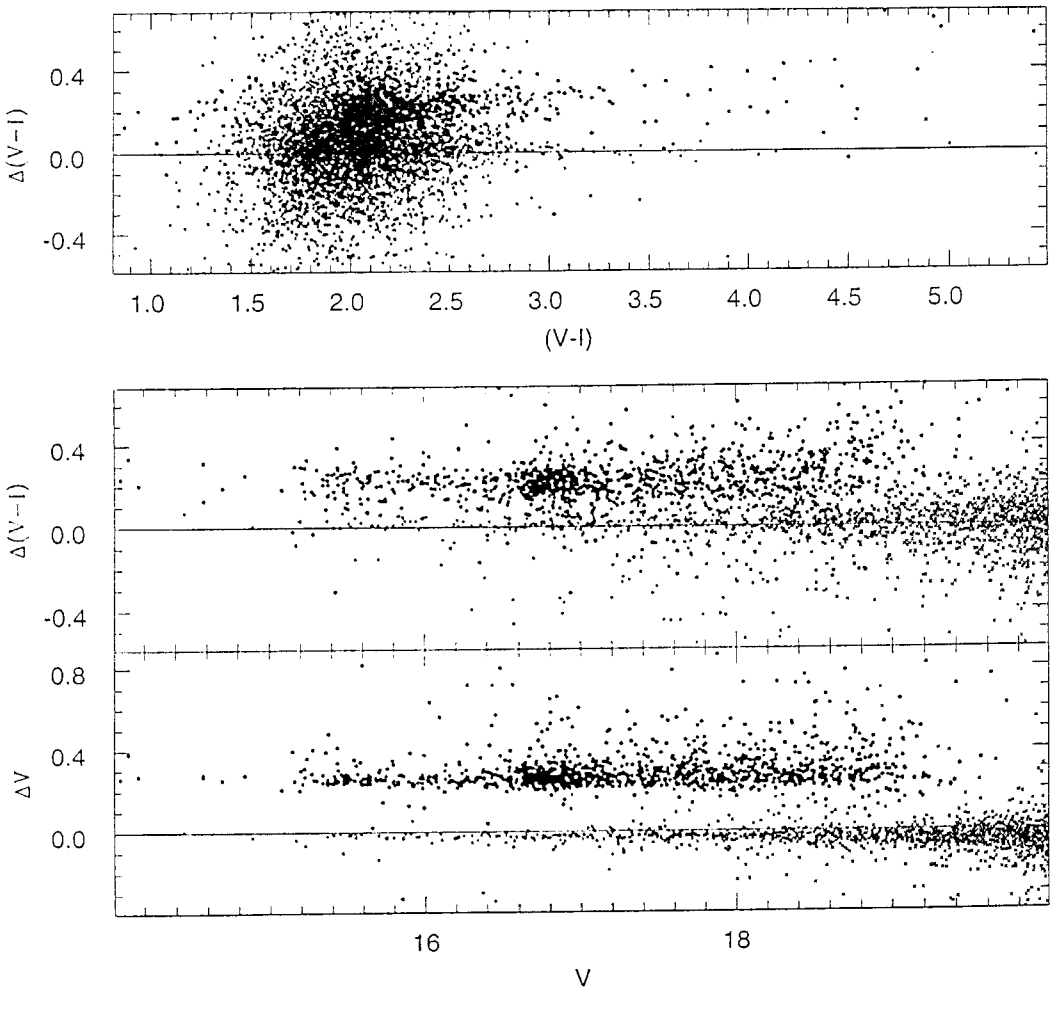

Fig. 2. Comparison of the present photometry with Ortolani et al. (1990) CCD data has been shown by filled circles. The differences are in the sense present minus their data, plotted against the present CCD photometry. Crosses denote the photometric comparison of the field region with the cluster region. The differences are in the sense cluster minus field data

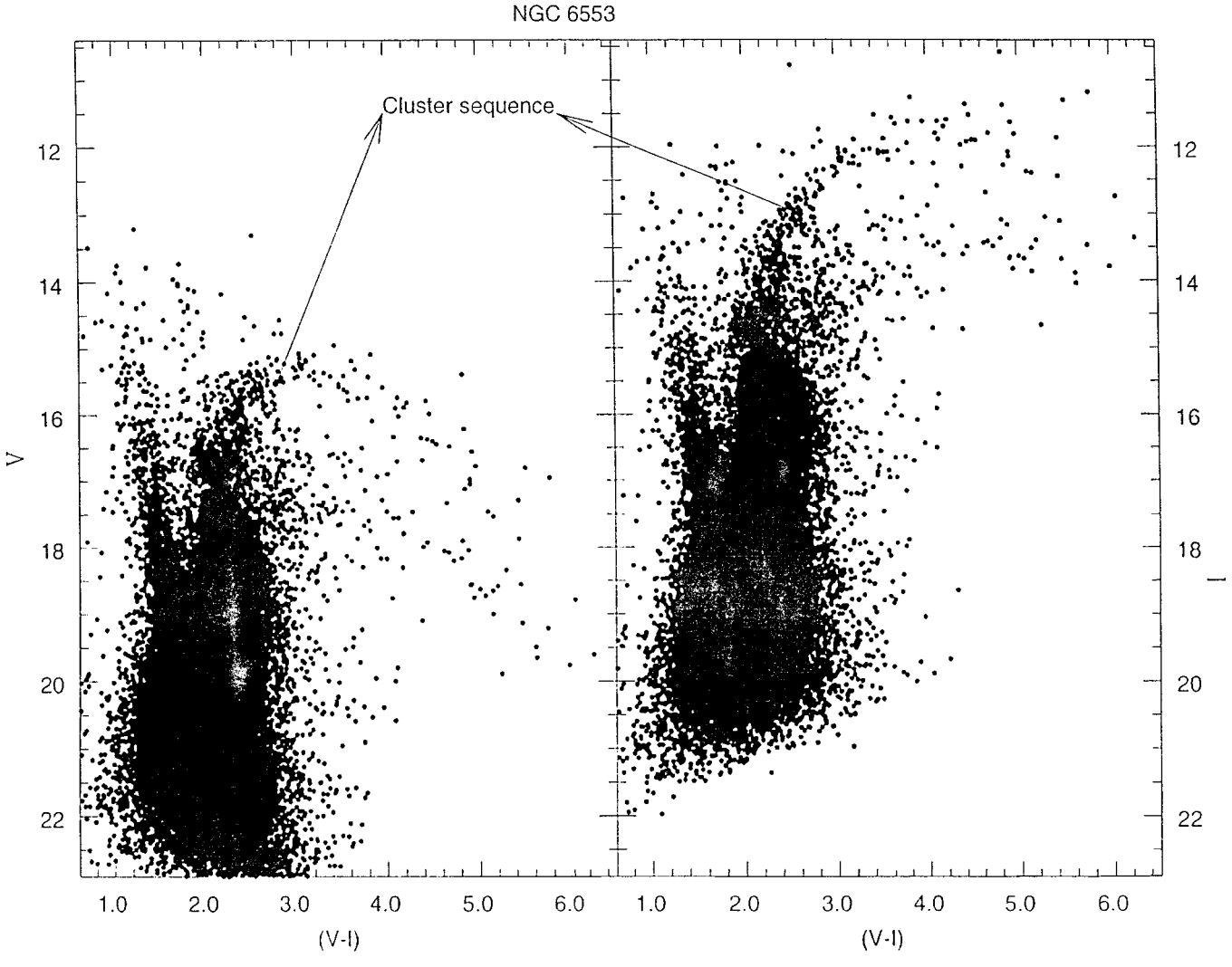

Fig. 3. The $V, (V-I)$ and $I, (V-I)$ diagram for all stars observed by us. The $(V-I)$ scale is compressed to show the presence of very red stars. Only for the brighter stars ($V \leq 18$), the cluster population can be distinguished from the rich population of field stars

indicating excellent agreement between the independent VI photometric data of the two regions.

However, a comparison of present photometry with Ortolani et al. (1990) indicates the following. Except for a few outliers, which appear to be mostly those that were treated as single in our measurements and as blended doubles in theirs, the distribution of the photometric differences seems fairly random with a constant zeropoint offset of ~ 0.3 mag in V and of ~ 0.2 mag in $(V-I)$. However, differences in colour $(V-I)$ are smaller for bluer objects and increase slightly for redder ones (see Table 3). A least-squares linear regression between the data points yields

$$\Delta(V-I) = 0.06(\pm 0.009)(V-I)_{\rm ccd} + 0.08(\pm 0.02)$$

with a correlation coefficient of 0.2. Obviously, there is a zeropoint difference in both V and I between the two sets of ground based CCD data. This is due to the difficulties encountered by Ortolani et al. (1990) in calibrating the data (see Guarnieriet al. 1998). The zeropoint offsets between HST data and ground based CCD data by Ortolani et al. (1990) found by Guarnieri et al. (1998) are similar to ours. This and the discussions in the sections to follow indicate that our photometry agrees fairly well with the HST data.

Now we turn to the results derived from the present VI CCD photometry.

4. Colour-magnitude diagrams

4.1. General remarks

Figure 3 shows the V, $(V-I)$ and I, $(V-I)$ diagrams of all 40 170 stars that were identified independently in both V and I filters. The CMD shows the difficulties present in

the study of cluster NGC 6553. The field population dominates in the fainter stars ($V \geq 18$) so much that the cluster sub-giant branch, MSTO region and MS itself are not visible at all. In the brighter stars, typical features of the field population in the direction of the Galactic centre and cluster RGB are clearly visible. The RGB of NGC 6553 is marked as cluster sequence in the Fig. 3. It turns over at about $V = 15.3, (V-I) = 2.9$ in the $V, (V-I)$ diagram. No such turnover is seen in the $I, (V-I)$ diagram. To the blue side of this sequence, the MS of the young Galactic disk stars can be easily identified while the older bulge populations are present towards the redder side. Both cluster and field populations contain a significant number of bright ($I \leq 15$) but very red stars with $(V - I) \geq 4.0$. These stars should be taken into account in population synthesis when interpreting red integrated colours of Galactic bulge populations.

4.2. Regions of cluster and field populations

Before discussing the features of cluster or field population any further it is essential to determine the regions in sky where one dominates over the other. In order to find out where the field population becomes dominant with respect to the cluster population we determined the radial stellar density profile of the region using stars brighter than $V = 20$ mag. The (X, Y) pixel coordinates of the eye-estimated cluster centre are (440, 645) with an accuracy of few arcsec. The observed stellar density profile up to $\sim 7'$ from the cluster centre is plotted in Fig. 4. The stellar densities derived here are not corrected for data incompleteness. They are therefore underestimated for inner regions (upto a radial distance of about $1'$), as the plot shown by Trager et al. (1995) indicates that data completness could be less than 50% in the central bin and reaches to $\sim 100\%$ only at about $1'$. Since the cluster profiles from star counts are better than those from integrated photometry in the outer regions, we have used the former for determining outer boundary of the dominant regions of the cluster population. The stellar density decreases strongly from cluster centre out to about a radius of $3'$. Beyond that it becomes asymptotic at a level of about 150 stars arcmin^{-2}. The profile given by King (1962) fits the observed stellar density profile satisfactorily.

The above analysis clearly indicates that the population of the cluster NGC 6553 is not dominant beyond a radial distance of $3'$ and most of the stars present in that part of the sky represent the field population. We therefore considered stars with $Y < 0$ pixels (outside the cluster frame; see Fig. 1), i.e., $\geq 215''$ from the cluster centre as representative of the field population. In order to maximise the percentage of cluster members in the sample and to avoid the effects of strong stellar crowding on the VI data, we consider only stars lying in an annular region (defined with inner and outer radii of 17

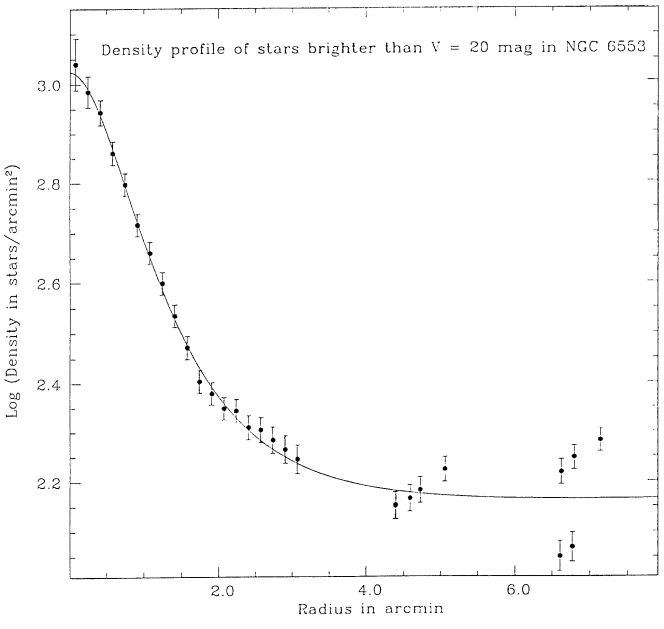

Fig. 4. This plot shows the observed stellar density (logarithm of stars brighter than $V = 20$ mag per square arcmin) as a function of radius in arcmin. The length of the bar denotes the error in density determination due to number statistics. The solid curve shows a least square fit of the King profile. The cluster population is not dominant beyond a radial distance of about $3'$

to 100 arcsec respectively) as representative of cluster population. The $V, (V - I)$ diagrams for the representatives of field and cluster populations are shown in Fig. 5. Their respective numbers are about 14 250 and 8 500. The corresponding areas are about 23.6 and 8.4 arcmin^2. The dominance of one population over other can be clearly seen in the both diagrams. With these better defined features of the two populations contamination effects in the CMDs stand out more clearly now. The limiting V mag of the field population is about a magnitude fainter than that of the cluster even though the exposure times are similar (see Table 1). This illustrates the effect of crowding on the limiting magnitude of the observations. We will now analyse both populations separately.

4.3. Subtraction of the field population

We have carried out statistical field star subtraction. For this, we consider only stars brighter than $V = 20$ mag in both cluster and field populations, since the cluster HB and RGB are present there. The field population used in the statistical subtraction has been selected from a rectangular region with coordinates (in pixels) $X = 0$ to 1000 and $Y = -725$ to -450. Thus the area is equal to that of the cluster region but located at a radial distance of about $7'$ from the cluster centre. At this radial distance, the cluster population will be negligible, as the values of core and tidal radii for the cluster are about $0.6'$ and $8'$

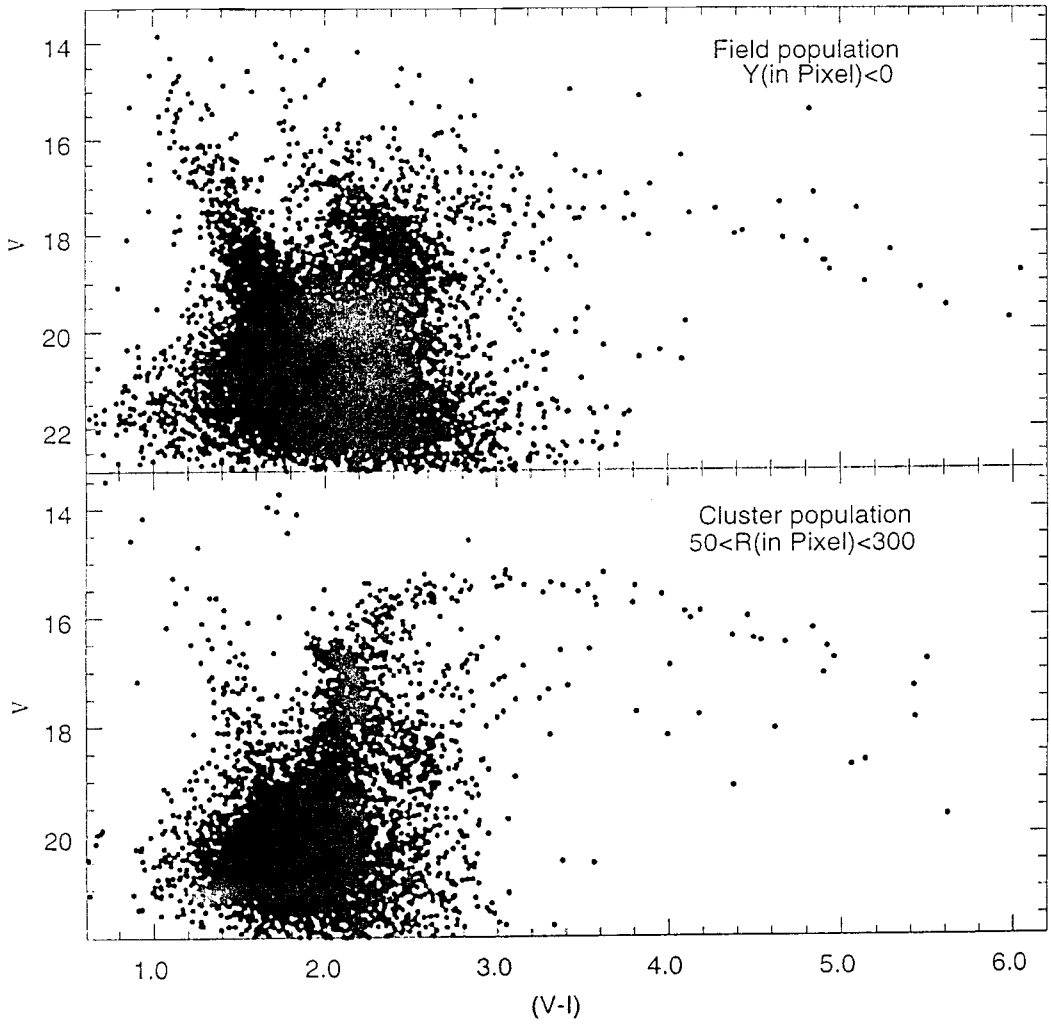

Fig. 5. The $V,(V-I)$ diagram for the representatives of cluster and field populations. The regions from where they were selected are listed. Dominance of one population over other can be clearly seen in these diagrams

respectively (cf. Trager et al. 1995). There are 3914 and 1317 stars brighter than $V = 20$ mag in the chosen cluster and field regions respectively. The statistical field star subtraction is done in the following manner. For each star of the field population, the nearest star located within a box of size ± 0.5 mag in V and ± 0.2 mag in $(V-I)$ from the $V,(V-I)$ position of the field star in the CMD of the cluster region is deleted from the sample. This procedure will remove statistically field stars from the selected cluster region. However, precisely because of this we cannot completely rule out the presence of some field stars in the cleaned sample or oversubtraction in the cluster data. The lower part of the Fig. 6 shows the CMD of the cleaned sample. The RGB and HB are very well defined in the diagram. Some field stars mostly right side of the cluster SGB are still present in the diagram but they will not affect the results.

5. The colour-magnitude diagram morphology and parameters of NGC 6553

5.1. Duration of the RGB-bump phase

Figure 7 shows the differential luminosity function of the GB branch derived from the field star subtracted sample of the cluster. There are two peaks marked in the histograms. The higher peak contains the HB stars while the smaller contains the stars belonging to the RGB-bump which is a clump of stars along the RGB evolutionary phase. This clump is due to a temporary reversal in the star path that is ascending the RGB, the star stops and goes toward slight fainter magnitudes for some time and then starts again ascending the RGB. In the $V,(V-I)$ diagrams of the Galactic bulge clusters, which have nearly solar

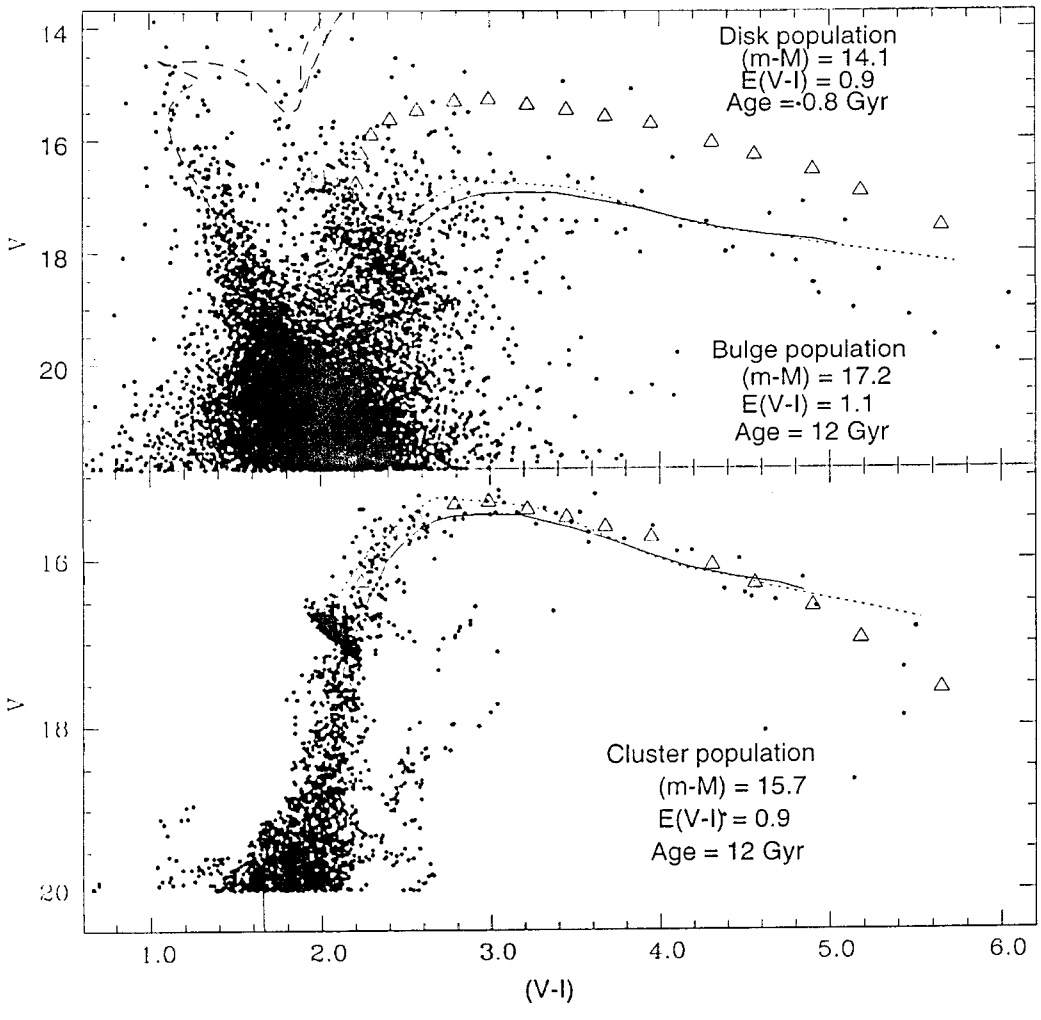

Fig. 6. The $V,(V-I)$ diagrams for the cluster and field stars are presented. The cluster population is for stars brighter than $V = 20$ mag. The sample has been cleaned statistically for the field star contamination. The field stars brighter than $V = 21$ are plotted. Theoretical isochrones from Bertelli et al. (1994) for solar metallicity are overplotted for indicated apparent distance modulus, reddening and age. The solid curve is the RGB while the dotted one traces the AGB. The dashed curve is the isochrone fitted to the disk population of the galaxy. The eye-estimated fiducial points for the RGB and HB are plotted by open triangles and squares respectively

metallicity, the RGB-bump is located below the HB (cf. Lanteri Cravet et al. 1997) and the same is observed for NGC 6553 in Fig. 7. This indicates that the cluster metallicity is nearly solar which is in agreement with the morphological features present in the $V,(V-I)$ diagram of the cluster (see discussions below).

The ratio of duration of the RGB-bump phase relative to the life time of the star during the HB phase for clusters having characteristics of the Galactic bulge clusters is 0.2 (cf. Lanteri Cravet et al. 1997 and references therein) and is equal to the ratio of number of stars present in the corresponding evolutionary phases. In order to carry out the star counts in the two evolutionary phases, we used the linear interpolation (see dotted line in the Fig. 7). We obtained the ratio of numbers in the RGB-bump and the HB phases as 0.17 ± 0.05 which is not too different from the value of 0.19 ± 0.03 obtained by Lanteri Cravet et al. (1997) for the cluster. Considering the uncertainty, one can say that the value is in good agreement with the theoretical predictions of 0.2.

5.2. Morphology of the horizontal branch (HB)

A very interesting feature in the lower $V,(V-I)$ diagram (Fig. 6) is the position of HB. It is very red, elongated, tilted, and even overlaps with the RGB. Such tilted and elongated HBs have been repeatedly reported for metal-rich clusters located towards the Galactic centre (see Ortolani et al. 1997; Grebel et al. 1995). Armandroff (1988) proposed differential reddening as the cause, because the slope of the tilted feature resembles in the most striking cases the reddening vector. For Terzan 5, Grebel

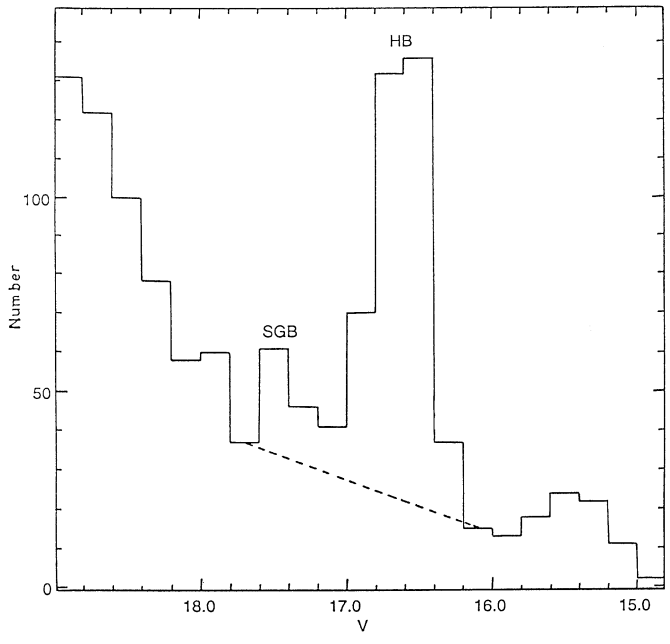

Fig. 7. The differential luminosity function of the GB. The peaks due to the HB stars and RGB-bump are marked as HB and SGB respectively

et al. (1995) showed that differential reddening is present, derived a reddening map, and dereddened the initially diagonal HB, which became clumpy and lost its diagonality almost entirely. Also the RGB became much narrower. A small amount of "diagonality" still remained, which may indicate that some of it is an intrinsic property of HB evolution as indicated by theoretical HB tracks. For the first time, it was shown directly that most of the diagonality is indeed caused by differential reddening. In order to understand the cause in the case of NGC 6553, we carried out following analysis:

(a) In order to derive an extinction map, we divided the observed cluster region into boxes of $\sim$ 200 $\times$ 200 pixels^2, as indicated in the Table 4 and identified the HB stars located in the box. The star is considered as a HB star if its brightness is $16.35 < V < 17.55$ and the colour is $1.85 < (V-I) < 2.35$. Theoretical models indicate that all HB stars have an (almost) equal luminosity but have range in temperature due to different shell mass. This fact is used to derive the extinction value for a box from the mean apparent brightness of its HB stars. For this, we used the results given by Guarnieri et al. (1998) that the apparent brightness of the HB stars of the cluster ($V_{\rm HB} = 16.92$) corresponds to $A_v = 2.34$. The value of A_v and the number of HB stars found in the box are listed in the table. Generally more than 5 HB stars are present in a box, except in the boxes with $X \geq 800$. The standard deviation (σ) of the mean V value of the HB stars in a box is generally $\sim$ 0.2. One finds that the values of A_v change smoothly along a column and randomly along the row with the minimum vaues in the row with $Y = 350$ to 550. This indicates presence of strong differential extinction in the north south direction of the cluster region. It is in agreement with the obscuration observed on the sky survey plate and also with the observations of Ortolani et al. (1990).

(b) In order to study variaton in shape and width of the HB and RGB across the cluster face, we plotted in Fig. 8 the $V, (V-I)$ values of the HB and RGB stars located in the six cluster regions. It clearly shows that both scatter as well as tilt of the HB differ from one region to other. Both the HB and RGB sequences in a region are narrow and well defined. This indicates that most of the scatter present in $(V-I)$ colour of the cluster RGB sequence (see Figs. 5 and 6) is due to presence of differential extinction across the cluster face. However, the HB of a region is always tilted and elongated. Presence of differential interstellar extinction across the face of a box (size $\sim 66'' \times 66''$) can not be ruled out, as radio studies indicate very small scale (a few AUs) patchy absorption in the Galactic disk. It may not be strong as its effect on the RGB (see Fig. 8) of a region in the form of scatter is not very large. This may indicate that presence of differential extinction across the cluster face may not explain the observed elongation of the cluster HB sequence. Further studies are desired for understanding them.

(c) In order to quantify the extent of differential extinction present across the cluster face, we plotted mean loci of the HB and GB sequences of the different cluster regions in Fig. 9. Average slope of the HB seems to be not too different from the normal slope of interstellar reddening. However, extent of elongation of the HB differs from one strip to other. The mean loci of the GB sequences of the regions with $Y = 150$ to 360; 350 to 550 and 550 to 750 are almost identical. However, the mean locus of the GB sequence of the region with $Y = 750$ to 950 is clearly shifted towards red side. This indicates that extent of differential reddening amounts to $\Delta E(V-I) \sim 0.2$ mag and $\Delta A_v \sim 0.5$ mag. This agrees very well with the results derived from the brightness of the HB stars (see Table 4). Ortolani et al. (1990) observed slightly smaller extent of differential extinction across the cluster region.

The above analysis indicates that presence of differential extinction across the cluster face can explain most of the scatter present in the RGB sequence of the cluster population. However, it may not explain more than a magnitude elongation observed in the V magnitude of HB stars of NGC 6553. Ortolani et al. (1990) suggest that blanketing effect can also produce tilting and extension in the HB of the cluster.

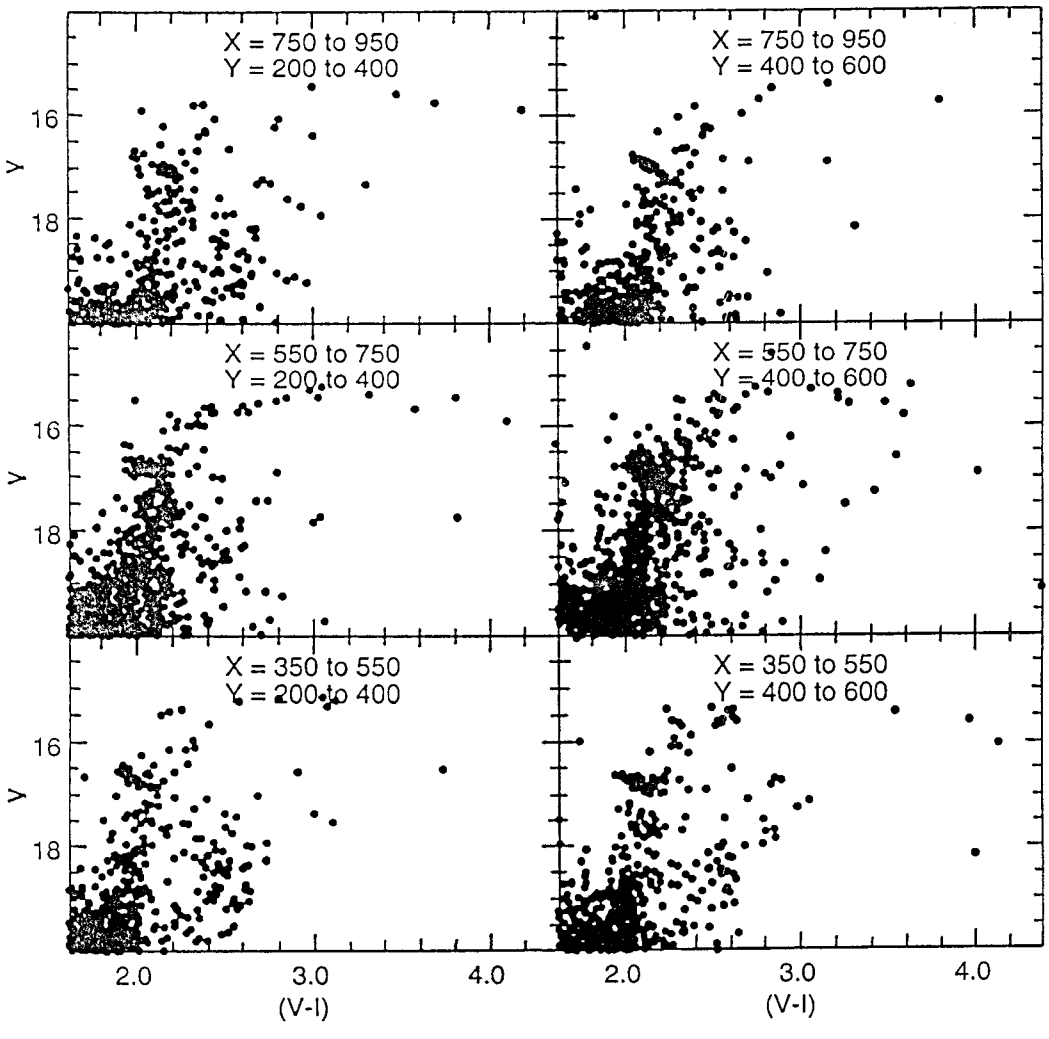

Fig. 8. The $V, (V-I)$ diagrams of the stars brighter than $V = 19$ mag located in the six rectangular strips of the central part of the cluster. The X and Y pixel coordinates of the strips are marked. The HB and RGB stellar sequences are clearly visible in all the diagrams

Table 4. Variation of extinction A_v across the face of the cluster NGC 6553. The number of HB stars observed in a box is given in brackets

Range in Y pixels	Range in X pixels				
	< 200	200 to 400	400 to 600	600 to 800	≥ 800
150 to 350	2.32(2)	2.31(10)	2.42(11)	2.52(3)	2.26(1)
350 to 550	2.06(13)	2.14(30)	2.19(32)	2.26(16)	2.21(8)
550 to 750	2.24(12)	2.30(76)	2.41(107)	2.29(21)	2.43(4)
750 to 950	2.41(8)	2.47(30)	2.48(34)	2.52(16)	2.01(1)
$\geq$ 950	2.50(3)	2.48(4)	2.59(5)	2.38(7)	2.50(2)

5.3. The morphology of the giant branch and cluster parameters

The lower part of Fig. 6 shows the presence of a well defined but broad RGB in the diagram. Eye-estimated fiducial points for the RGB and the HB are plotted in the figure and listed in the Table 5. Presence of differential extinction across the cluster face has been considered in this process. An error of ~ 0.03 mag in $(V-I)$ of the fiducial points of RGB is expected. The RGB is extended and curved down, characteristic of a nearly solar metallicity population, like that of the globular clusters NGC 6528, Terzan 5, Terzan 6, and Baade's window.

A theoretical isochrone from Bertelli et al. (1994) is overplotted in Fig. 6 for an apparent distance modulus of

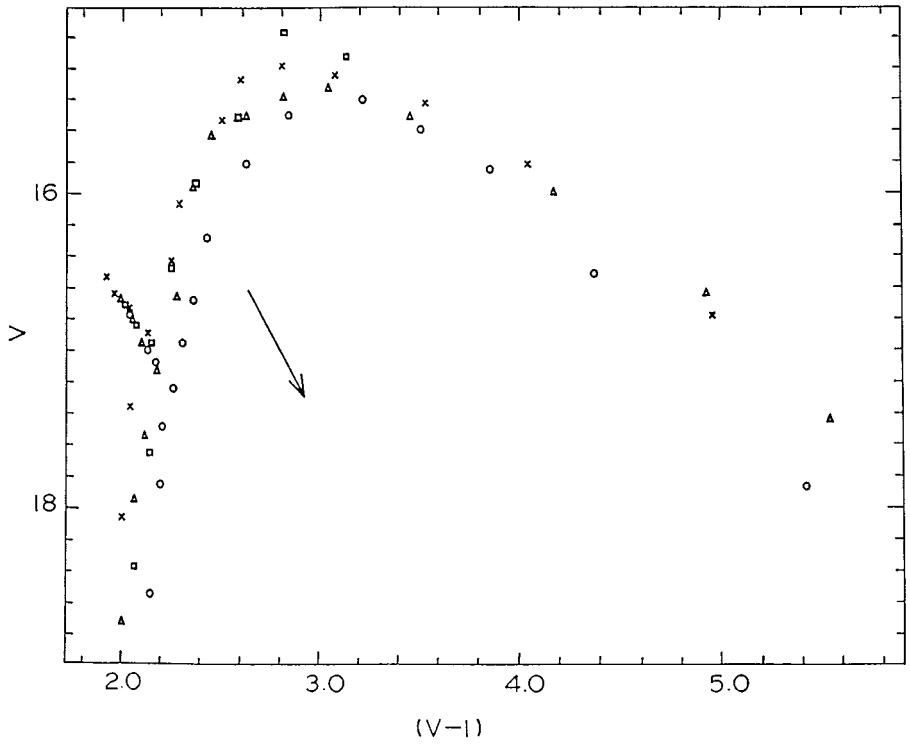

Fig. 9. The $V, (V-I)$ diagrams of the mean loci of the HB and GB sequences observed in different strips of the cluster region. Open squares, crosses, open triangles and open circles denote the fiducial points in the strips with $Y = 150$ to 350; 350 to 550; 550 to 750 and 750 to 950 respectively in the cluster region. The arrow indicates the direction of normal interstellar reddening vector

15.7 and reddening $E(V-I) = 0.9$. The isochrone has $Z = 0.02$ and an age of 12 Gyr. From the fitting of the theoretical isochrones in Fig. 6, one may say that the redder bright stars, if they are indeed cluster members, are on the AGB rather than in the RGB stage of stellar evolution. However, the evolutionary status of the red stars with a $(V-I)$ colour in the range of 3.5 to 5 is not clear as the isochrones for both AGB and RGB merge. The theoretical isochrone fits the shape of the observed RGB very well up to $(V-I) \sim 4.5$ and starts to deviate for redder colours. Similarly the theoretical isochrones cannot explain the location of the bright red stars observed in the $V, (V-I)$ diagram of NGC 6528 (see Richtler et al. 1998). This red extension of the AGB/RGB stars must be taken into account when modelling spectra of elliptical galaxies (see Bruzual et al. 1997, and references therein for a detailed discussion).

5.3.1. Metallicity and reddening

A number of spectroscopic analyses indicate that metallicity of the cluster NGC 6553 is close to solar. The [Fe/H] values range from −0.1 to −0.4 (see Rutledge et al. 1997; Origlia et al. 1997; Bruzual et al. 1997 and refernces therein). In order to check the consistency with these, we used the present photometric indicators for estimating the metallicity of NGC 6553. The morphology of the RGB can be used to estimate the metallicity and reddening of the cluster. Ortolani et al. (1991) used the slope of the RGB to determine abundances of the metal-rich globulars and found that the metallicity of NGC 6553 is similar to solar. Another indicator of the metallicity is the V magnitude difference between the HB level and the top (brightest) of the RGB, ΔV. Its value decreases with increasing metallicity of the cluster. Use of such relations avoids the otherwise required a priori knowledge of reddening for the determination of the metallicity of a cluster. Barbuy et al. (1997) find that the value of ΔV is 3.1 for NGC 7099 ([Fe/H] = −2.1), 2.3 for 47 Tuc ([Fe/H] = −0.7), 2.1 for NGC 6356 ([Fe/H] = −0.4) and 1.4 for NGC 6528 ([Fe/H] = −0.2). For NGC 6553, $\Delta V = 1.5 \pm 0.1$. This would place NGC 6553 with a nearly solar metallicity similar to NGC 6528 (cf. Barbuy et al. 1998).

Heitsch & Richtler (1999) have derived the following empirical relation between ΔV and [Fe/H] using theoretical isochrones given by Bertelli et al. (1994) for [Fe/H] = 0.4, 0.0, −0.4 and −0.7.

$$[\mathrm{Fe/H}] = (-0.57 \pm 0.03) \cdot \Delta V + (0.74 \pm 0.04).$$

This yields a value of -0.1 ± 0.1 for [Fe/H] of NGC 6553. This agrees very well with our above estimate as well as with earlier metallicity determinations for the cluster (see Bruzual et al. 1997;

Table 5. The fiducial sequence for the RGB and HB of NGC 6553

$(V-I)$	V	Sequence
5.65	17.56	RGB
5.18	16.95	
4.90	16.56	
4.56	16.29	
4.31	16.07	
3.95	15.73	
3.68	15.60	
3.45	15.48	
3.22	15.39	
2.99	15.29	
2.79	15.32	
2.57	15.48	
2.41	15.65	
2.30	15.92	
2.24	16.26	
2.21	16.78	
2.18	16.98	
2.15	17.50	
2.08	18.05	
2.06	18.32	
2.04	18.67	
1.96	19.14	
1.86	19.56	
1.80	19.88	
1.99	16.64	HB
2.07	16.77	
2.16	16.98	

Rutledge et al. 1997; Origlia et al. 1997; Guarnieri et al. 1998).

Richtler et al. (1998) have derived empirical relations between $(V-I)_0, g$ (intrinsic $(V-I)$ colour of the RGB at the magnitude level of HB in the CMD) and [Fe/H] using the $(V-I)$ theoretical isochrones given by Tripicco et al. (1995) and by Bertelli et al. (1994) for old and metal-rich clusters. We have used these to derive a $(V-I)_0, g$ value for the metallicity of NGC 6553. For $(V-I)_0, g$ the relation based on Tripicco et al.'s (1995) isochrones yields a value of 1.1 while the relation obtained using Bertelli et al. (1994) isochrones gives 1.3. A similar difference was found for NGC 6528 also (Richtler et al. 1998). This shows the uncertainty involved in the determination of $(V-I)_0, g$ using appropriate published theoretical isochrones which depends on the opacities and composition used in the models (see Salaris & Weiss 1998; Alonso et al. 1997, for a detailed discussion). There is growing evidence that alpha elements in the bulge are significantly enhanced in comparison to the values used in the theoretical stellar evolutionary models. Also, the transformations from the theoretical $M_{\rm bol}$ and $T_{\rm eff}$ to the observational visual magnitudes and colours are very uncertain at the low temperatures of the giant and subgiant stars in an old metal rich population. All these seem to be responsible for the observed 0.2 mag difference between the $(V-I)_0, g$ values derived from the isochrones of Bertelli et al. (1994) and Tripicco et al. (1995). In the present analysis, we have therefore used the mean 1.2 as a value for $(V-I)_0, g$. The observed value of this parameter in Fig. 6 is 2.15 ± 0.1, indicating a value of 0.95 ± 0.15 for the colour excess $E(V-I)$. This agrees fairly well with the value of $E(V-I) = 0.9$ obtained by us by fitting the theoretical isochrones to the shape of the RGB and with most of the earlier estimates of the reddening (see Barbuy et al 1998; Guarnieri et al. 1998 and references therein). We therefore adopted a value of $E(V-I) = 0.95$ in our further analysis.

5.3.2. Distance

For distance determination, we have used the following empirical relation between HB brightness and metallicity given by Salaris & Weiss (1998)

$M_V = 0.17 * [\mathrm{Fe/H}] + 0.78.$

This relation is consistent with the **HIPPARCOS**-based distance measurements and yields a value of 0.76 mag for M_V of NGC 6553. The mean brightness level for the HB stars of NGC 6553 is at $V = 16.7 \pm 0.2$ (see Fig. 7). This gives 13.7 as a value for the true distance modulus of NGC 6553, assuming a normal value of 2.37 for the ratio $A_V/E(V-I)$. However, if one takes into consideration that the absorption depends on the temperature, surface gravity and metallicity of the star considered, as was studied recently by Grebel & Roberts (1995), then the value of the ratio becomes 2.6 and a slightly lower value of 13.5 mag is derived for the true distance modulus of the cluster. Considering all these uncertainties, one can say that the cluster is located at a distance of about 5 kpc from us and ~ 3 kpc from the Galactic centre at the outer fringe of the bulge. The present distance estimate agrees very well with the values given recently by Ortolani et al. (1995) and by Guarnieri et al. (1998).

5.4. Parameters of the field population

The $V, (V-I)$ diagram for the brighter field stars ($V < 21$) is shown in the upper part of Fig. 6. Some stars belonging to the cluster population are also present, but they will not affect the results. The blue MS of Galactic disk stars and the bulge RGB and HB stars dominate the diagram, and the cluster sequence is too sparse to be identified. The CMD is very similar to that of Baade's window and those of the other fields near the Galactic centre published recently by Paczynski et al. (1994) and earlier by Terndrup (1988). In order to estimate reddening, distance and age of the relatively narrow and well defined MS, we fitted Bertelli et al. (1994) isochrones for solar metallicity and found $(m-M) = 14.1 \pm 0.3, E(V-I) = 0.9 \pm 0.05$

and age = 800 $\pm$ 200 Myr. Paczynski et al. (1994) have also observed this population almost at the same distance of $\sim$ 2 kpc. At this distance, along the line of sight, the scale height of the thin disk corresponds to a distance of $\sim$ 100 pc. All these indicate that the foreground stars are in the Galactic disk and they are concentrated at a single distance of $\sim$ 2 kpc. The dispersed but clearly defined RGB and the tilted and elongated ($\Delta(V-I) > 0.7$ mag) HB are in part caused by depth effects along the line of sight and probably also by differential interstellar extinction within the field region. The slope of the HB tilt is $\sim$ 2.5. The RGB of the bulge populations also turns over just like the NGC 6553 population. In Fig. 6, a theoretical isochrone from Bertelli et al. (1994) is overplotted for apparent distance modulus of 17.2 and reddening $E(V-I) = 1.1$. The isochrone has $Z = 0.02$ and an age of 12 Gyr. The fits of theoretical isochrones in Fig. 6 cannot account for the bright stars with $(V-I) \geq 4.5$ as seen also in the cluster population. There are about 10 such stars.

The location of the HB and the morphology of the RGB have also been used to estimate distance, reddening and metallicity of the bulk of the bulge populations present in the direction of the cluster. For this, we have used NGC 6553 as a reference. The value of ΔV, the magnitude difference between the HB level and the top (brightest) of the RGB in V is 1.5 $\pm$ 0.2 indicating nearly solar metallicity for most of the bulge populations. The location of the HB where it joins the RGB is about 1.5 $\pm$ 0.4 mag fainter in V and about 0.3 $\pm$ 0.2 mag redder in $(V-I)$ than the corresponding location of NGC 6553 in the V, $(V-I)$ diagram. It means that most of the bulge stars in the direction of the cluster are background stars located at distances larger than $\sim$ 7 kpc with reddening $E(V-I) \geq 1.2$. These estimates agree fairly well with the values derived from the isochrone fitting.

6. Discussion and conclusions

We have carried out VI CCD photometry of about 40 000 stars down to $V = 23$ mag. They are located in an area of about 6×10 arcmin^2 in the direction of the cluster NGC 6553. Our photometric zeropoint calibrations agree fairly well with the HST data. Present observations have derived the parameters for the field population present in the direction of the cluster for the first time. These indicate that NGC 6553 is situated behind the young ($\sim$ 800 Myr) population of the Galactic disk but in front of most of the bulge stars. The young population located at a distance of $\sim$ 2 kpc suffers in interstellar extinction of $A_v \sim 2.2$ mag. This is consistent with the average standard interstellar absorption in the disk of $\sim$ 1 mag/kpc adopted in many studies of galactic structure (cf. Neckel & Klare 1980 and references therein). This indicates that there is almost no interstellar matter present between the young population of the Galactic disk and the cluster, as both have almost similar interstellar extinction with $E(V-I) \sim 0.9$ mag. This is in accordance with the structure of Galactic thin disk, because, along the line of sight, at the distance of young population, we are leaving the thin disk where the dark clouds are concentrated.

The morphology of the RGB corrected for field star contamination confirms the nearly solar metallicity for the cluster population determined spectroscopically. Tilt and elongation in the HB of cluster population can not be understood in terms of the presence of differential extinction across the cluster region.

Acknowledgements. We gratefully acknowledge the useful discussions with K.S. de Boer and V. Mohan. A. Dieball helped in field star subtraction. The valuable suggestions given by anonymous referee has improved the paper significantly. The financial support provided by the Alexander von Humboldt Foundation to RS is gratefully acknowledged. TR wants to thank the Alexander von Humboldt Foundation for generous support and the Indian Institute of Astrophysics, Bangalore for hospitality and financial support. EKG acknowledges support by the German Space Agency (DARA) (grant 05 OR 9103 0) and by Dennis Zaritsky through NASA LTSA grant NAG-5-3501. Furthermore, we thank S. Ortolani for mailing his ground based CCD photometric data. This research has made use of the SIMBAD database, operated at CDS, Strasbourg, France.

References

Alonso A., Salaris M., Martinez-Roger C., Straniero O., Arribas S., 1997, A&A 323, 374
Armandroff T.E., 1988, AJ 96, 588
Barbuy B., Bica E., Ortolani S., 1998, A&A 333, 117
Barbuy B., Castro S., Ortolani S., Bica E., 1992, A&A 259, 607
Barbuy B., Ortolani S., Bica E., 1997, A&AS 122, 483
Bertelli G., Bressan A., Chiosi C., Fagotto F., Nasi E., 1994, A&AS 106, 275
Bruzual G., Barbuy B., Ortolani S., Bica E., Cuisinier F., Lejeune T., Schiavon R.P., 1997, AJ 114, 1531
Grebel E.K., Roberts W.J., 1995, A&AS 109, 293
Grebel E.K., Brandner W., Richtler T., Subramaniam A., Sagar R., 1995, BAAS 27, 1404
Guarnieri M.D., Montegriffo P., Ortolani S., Moneti A., Barbuy B., Bica E., 1995, The Messenger 79, 26
Guarnieri M.D., Ortolani S., Montegriffo P., Renzini A., Barbuy B., Bica E., Moneti A., 1998, A&A 331, 70
Hartwick F.D.A., 1975, PASP 87, 77
Heitsch F., Richtler T., 1999 (in preparation)
King I.R., 1962, AJ 67, 471
Landolt A., 1992, AJ 104, 340
Lanteri Cravet F., Guarnieri M.D., Renzini A., Ortolani S., 1997, Advances in stellar evolution, Rood R.T., Renzini A. (eds.), p. 59
Lloyd Evans T., Menzies J.W., 1973, in Variable stars in Globular Clusters and in Related Systems, IAU Col. 21, Fernie J.D. (ed.). D. Reidel Publishing Co., p. 151

Neckle Th., Klare G., 1980, A&AS 42, 251
Origlia L., Ferraro F.R., Fusi Pecci F., Oliva E., 1997, A&A 321, 859
Ortolani S., Bica E., Barbuy B., 1997, A&A 326, 614
Ortolani S., Barbuy B., Bica E., 1990, A&A 236, 362
Ortolani S., Barbuy B., Bica E., 1991, A&A 249, L31
Ortolani S., Renzini A., Gilmozzi R., Marconi G., Barbuy B., Bica E., Rich R.M., 1995, Nat 377, 701
Paczynski B., Stanek K.Z., Udalski A., Szymanski M., Kaluzny J., Kubiak M., Mateo M., 1994, AJ 107, 2060
Richtler T., Grebel E.K., Subramaniam A., Sagar R., 1998, A&AS 127, 167
Rutledge G.A., Hesser J.E., Stetson P.B., 1997, PASP 109, 907
Salaris M., Weiss A., 1998, A&A 335, 943
Stetson P.B., 1990, PASP 102, 932
Stetson P.B., 1992, in IAU Coll. 136, Stellar photometry – current techniques and future developments, Butler C.J. & Elliott I. (eds.), p. 291
Trager S.C., King I.R., Djorgovski S., 1995, AJ 109, 218
Terndrup D.M., 1988, AJ 96, 884
Tripicco M.J., Bell R.A., Dorman B., Hufnagel B., 1995, AJ 109, 1697
Zinn R., 1985, ApJ 293, 424